8-2012

# Measurement-driven performance analysis of indoor femtocellular networks

Trung-Tuan LUONG
*Singapore Management University*, ttluong@smu.edu.sg

Vigneshwaran SUBBARAJU
*Singapore Management University*, vigneshwaran@smu.edu.sg

Archan MISRA
*Singapore Management University*, archanm@smu.edu.sg

Srinivasan SESHAN
*Carnegie Mellon University*

## Citation

# Measurement-Driven Performance Analysis of Indoor Femtocellular Networks [*]

Trung-Tuan Luong,Vigneshwaran Subbaraju, Archan Misra
School of Information Systems
Singapore Management University
{ttluong,vigneshwaran,archanm}@smu.edu.sg

Srinivasan Seshan
School of Computer Science
Carnegie Mellon University
srini@cs.cmu.edu

## ABSTRACT

This paper describes initial empirical studies, performed on a 6-node 3G indoor femtocellular testbed, that investigate the impact of pedestrian mobility on network parameters, such as handoff behavior and data throughput. The studies establish that, owing to the small radii of cells, even modest changes in movement speed can have disproportionately large impact on handoff patterns and network throughput. By also revealing a strong temporal dependency effect, the studies motivate the need for algorithms to accurately predict RF signal strength distributions in dynamic indoor environments. We present such an RF prediction algorithm, based on crowd-sourced signal strength readings, and show that the algorithm can predict RF signal strengths with an average estimation error of $\pm 3$ dBm.

## Categories and Subject Descriptors

C.2.1 [**Network Architecture and Design**]: *Distributed networks; Wireless communication*

## Keywords

Femtocellular, Crowd-sourcing, RF signal

## 1. INTRODUCTION

Small-cell (loosely referred to as *femtocells*) overlay architectures hold the promise of significantly increasing the available wireless broadband capacity, especially in highly-trafficed public indoor spaces (such as shopping malls, subway stations and college/office buildings). The smaller cell sizes enable much higher spatial reuse of available spectrum and allow mobile devices to achieve higher data throughputs at lower transmission power. Besides introducing well-known issues of macro-femto interference [5], the smaller cell

sizes (typical cell radii of commercial femtocell access points (**FAPs**) vary between 8-20 meters) also imply a higher sensitivity to *user mobility*.

The *LiveLabs* project [1] is building an advanced wireless network testbed at multiple public places in Singapore, including the SMU campus, to enable testing of a variety of advanced lifestyle-based mobile applications and services on a 30,000 strong set of participating consumers. To enable experimentation with next generation high bandwidth, rich-media applications (such as HD-quality video conferencing and multimedia mobile gaming), we are exploring the deployment of an extensive (200-250 FAPs across 5 campus buildings) 3G/4G femtocellular network on the SMU campus.

Our eventual goal is to support 2 Mbps bi-directional throughput per user, simultaneously for 200 users collocated in a public venue, such as the university auditorium. Supporting such high capacity is specially difficult due to the highly *uneven demand distribution*, arising from spatiotemporal assymetry in user densities at different campus locations. As provisioning for such spatiotemporally-skewed peak demand is simply economically infeasible, we are exploring techniques to optimally utilize the combined available bandwidth across multiple access networks (macrocells, femtocells and Wi-Fi). Accordingly, an important research objective is to develop better user management algorithms that dynamically assign subscribers to the femto underlay or the macrocellular (3G/LTE) overlay, taking into account *individualized context*, such as a person's movement characteristic & the QoS demands of the active application on her mobile device.

To gain a deeper, empirical understanding of the performance characteristics expected of this advanced network, we have deployed (in partnership with a major telecom operator) a 6-node 3G femtocellular network across 2 floors of the School of Information Systems (SIS) building on the SMU campus. In this paper, we use this network to first investigate the role that differences in individual context (more specifically, the *variation in pedestrian movement speeds*) have on the network performance observed by mobile devices. Specifically, we use an extensive set of longitudinal experiments and observations to establish the sensitivity of two parameters: *a)* the handoff behavior across FAPs, and *b)* the throughput of mobile data traffic, on changes in the *indoor pedestrian movement speeds*. Our longitudinal studies not only demonstrate the significant impact that such movement speed variations have on the handoff behavior and the data throughput, but also reveal that the behavior has *sig-*

nificant temporal (time-of-day and across-days) variation as well. In particular, our measurements show that changes in indoor RF propagation can result in $\approx 10 - 15 \text{dBm}$ variation in AP signal strength measurements at different indoor locations.

To predict and manage the handoff behavior of mobile devices in such an indoor environment, it is thus necessary to predict *in near-real time* the RF environment (and the resulting FAP signal strengths) at different locations inside the building. Accordingly, we next propose and develop an innovative 'crowd-sourcing' based RF estimation algorithm, which uses the (signal strength vector, location coordinate) tuples reported by mobile devices to then determine the predicted signal strengths at other locations. Using unsupervised clustering and estimation techniques, our algorithm is able to predict the RF signal strengths at uncalibrated locations with an average error of only 3.3 dBm. We believe that such a 'crowd-sourced' estimation approach is especially promising, as its accuracy increases with an increase in the number of observation points (i.e., the number of mobile devices located in the indoor space), and is thus especially effective at predicting femtocellular network behavior when user density (and demand) exhibits peaks.

**Key Contributions:** We believe that this paper makes the following two key contributions:

- It uses real-life measurement studies to demonstrate that both handoff behavior and data traffic throughput characteristics of femtocellular networks are heavily influenced by the variation in indoor pedestrian movements. While this claim may be generally true for all cellular networks, we show that our variations are much more acute for femtocellular environments due to the smaller cell sizes (which greatly increases the frequency of mobility-induced cell transitions).

- It proposes an unsupervised approach to real-time RF prediction in indoor environments. The approach assumes that indoor propagation effects are captured by a log-distance path loss model and first tries to cluster those (not necessarily contiguous) areas that have similar model parameters, and then uses genetic algorithm-based optimization to best estimate the parameters for each of these clusters. Real-life measurements demonstrate that this approach is quite accurate in predicting indoor RF signal strengths.

The rest of this paper is organized as follows. Section 2 describes related work that influences and motivates our research. Next, Section 3 describes the key features of our 6-FAP testbed. Section 4 then presents the results on the impact of movement speed variation on (handoff, throughput) parameters. Section 5 then presents our real-time RF prediction and describes the performance results. Finally, Section 6 concludes the paper and describes ongoing work and open challenges.

## 2. RELATED & BACKGROUND WORK

Much of the literature related to the operational optimization of femtocells has focused on the problem of *interference management*, which assumes that the FAPs and the macrocellular base stations (BTS) operate on a common frequency band. For example, the CTRL framework [12]

employs a slower-control loop to protect a macrocell's uplink traffic from interference caused by multiple FAPs located in the vicinity and faster-timescale power control to protect a femtocell user from bursty macrocellular transmissions, whereas the power control scheme in [6] proposes a utility-based SINR adaptation approach (where each FAP adjusts its power so as to maximize an objective function that has a penalty proportional to the interference at the macrocell BTS). Femto-macro interference management is a non-issue in our femtocellular testbed, where the *FAPs and the macrocells are allocated separate frequency bands by the telecom operator.*

The problem of handoff management between femtocells and an overlay of macrocells was studied in [11], which proposed (as expected) that slow moving users should handoff within femtocells whereas fast moving users should preferentially utilize the macrocellular network. To reduce the number of handoffs encountered while transiting smaller-sized cells, [4] proposes an adaptive hysteresis threshold approach, where the handoff threshold is lowered as the user location approaches the edge of a cell boundary. This approach does not consider the difference in movement speeds of different users. Likewise, [13] investigates how the user's movement speed and application QoS requirements can be used to switch a user between a macrocell and femtocellular network. All of these approaches principally apply for outdoor environments (as they implicitly assume the availability of GPS-based estimates of user movement speed); moreover, their performance results are based on simulations and have not been empirically validated on a real testbed.

The problem of constructing an RF Map for indoor environments based on measured signal strengths was first studied in [9], which proposed the TIX algorithm that used inter-AP measurements of RSSI values to predict the RSSI readings at intermediate points based on *linear interpolation.* However, [9] did not study the problem of temporal variation of signal strengths in public indoor spaces. The ARIADNE framework [10] tackles the RF construction problem from a different perspective, using a two-dimensional floor plan and ray tracing (along multiple paths) of signals from a previously calibrated Wi-Fi AP to compute the unknown signal strength at different places. While experimental results showed that the estimation error was within $3\% - 5\%$ of the maximum RSSI, an approach such as ARIADNE considers only 2-D propagation and ignores the fact that the indoor environment can vary *significantly over a short time span*-e.g., doors to a classroom may be left open or closed, ferromagnetic equipment may be set up for exhibits/kiosks in the student concourse, etc.

Our work on real-time 'crowsourcing-based' estimation of RF properties is inspired by the work [7] in building the EZ localization system. In particular, the EZ algorithm assumes a log-distance path loss model (**LDPM**) between indoor APs and mobile devices, and uses multiple simultaneous RSSI measurements from the various mobile devices to estimate both the parameters of the log-distance model and the *locations* of the APs. In contrast to the goals of EZ, our aim is not to localize the mobile nodes, but instead to create an appropriate RF map (i.e., appropriate choice of parameters in the LDPM) and thereby *predict the signal strength* values at other locations (for which no recent measurements exist) within the indoor environment. Thus, before applying an optimization algorithm to estimate the LDPM models for
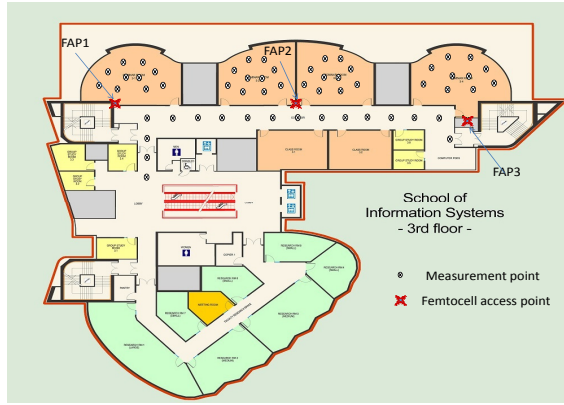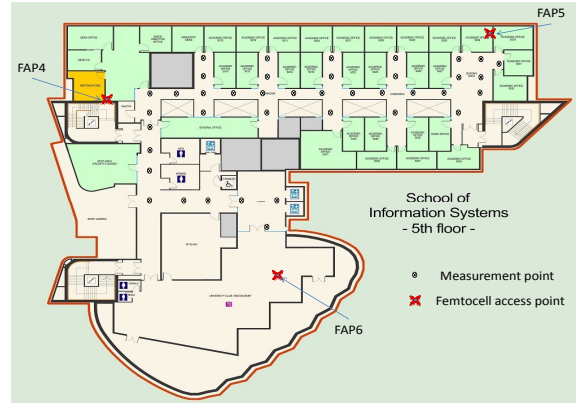
a. Floor 3                                    b. Floor 5

Figure 1: Floor layout, Femtocell deployment and measurement points

a set of measurements with the same propagation behavior, we must *first also determine the number of distinct RF environments within the indoor space.*

## 3. TESTBED AND EXPERIMENTAL SETUP

As mentioned before, our experimental testbed consists of 6 commercially available FAPs (Huawei ePico3801B) deployed across 2 floors of the SIS building on the SMU campus. The femtos support HSPA-based data transfers with peak rate of 7.2 Mbps downlink and 1.9 Mbps uplink, and operate on the 2.1GHz band, using FDD to support shared access by multiple users. Each of the femtos has a maximum capacity of 8 simultaneous voice and 16 simultaneous data connections. It is important to note that, consistent with our telecom operator's deployment strategy, our FAPs were configured to operate on a frequency band that is *isolated* from the macro-cellular bands–in other words, our testbed is essentially free from macrocellular interference.

Each floor had 3 of the femtos, deployed in static positions (their positions remain unchanged from the initial deployment), by the telecom operator with the initial goal of completely covering the entire floor space of the $5^{th}$ floor and the public half of the $3^{rd}$ floor. The FAPs on the $3^{rd}$ floor were placed inside lecture/seminar halls (see Figure 1a.), while the FAPs on the $5^{th}$ floor were placed in a mixture of different locations (faculty offices, research center & Dean's office), as shown in Figure 1b. The $3^{rd}$ floor deployment experienced more variable human traffic (with seminar halls having widely varying student densities); moreover, opening or closing the doors of these lecture halls causes variations in the signal power along the corridors. The FAPs on the $3^{rd}$ floor have overlapping coverage area (with all three FAPs visible at certain locations). In contrast to the $3^{rd}$ floor, the $5^{th}$ floor has less variation in human traffic (as it is typically off limits for students and houses research and faculty staff). While Line-Of-Sight free space propagation between $3^{rd}$ & $5^{th}$ floor is ostensibly not possible due to the intervening floors, the floor layouts have some "open space" at the edges of all the floors, allowing reflected propagation. As a result, some of the FAPs from one floor are 'visible' at certain specific points on the other floor.

To associate our measurements (of signal power RSCP, signal quality Ec/No and throughput) with location 'ground truth', we marked 57 specific points (approximately 2.5m apart) on the $3^{rd}$ floor covering both the corridor and the seminar room seating area, and 40 different points (approximately 3m apart) along the corridors of the $5^{th}$ floor. All the FAPs were configured to operate on full power (100 mW).

All the measurements of both RF strengths and application throughput were performed on the mobile device side using the Nemo Outdoor tool (v5.8) [2]. The data throughput measurements (which involved the download of large-sized files using *ftp*) were made with a Qualcomm 5250 USB 3G-Modem attached to the laptop, while voice calls measurements were made with a Nokia 6680 phone (that was equipped with custom built firmware for Nemo Outdoor). It is worth noting that laptop/phone models were identical to the ones used by the telecom operator for their signal power site survey. In addition to those Nemo-specific devices, we also carried along 2 Android phones during our measurement walkabouts, and used the Android APIs to log the signal readings on those phones.

## 4. HANDOFF AND THROUGHPUT DEPENDENCY ON MOVEMENT

We now describe our initial experiments that studied the impact of different pedestrian movement speeds on two important parameters: *a)* handoff and *b)* data throughput. To conduct this study, we had two participants walk along a pre-specified trajectory at three different specific speeds $\{Slow, Normal, Fast\}$. The specification was descriptive– i.e., instead of an absolute value, the participants were instructed to walk at, or slower/faster than, their 'normal' pace. Simultaneously, we tracked the 'ground truth' of their movement, at the granularity of the 'specific points', by noting the timestamps at which they transited these points.

We measured the RSCP and Ec/No parameters under two usage conditions, one with an active voice call, and the other with an active downlink ftp-based data transfer. The participants repeated thease measurements at different times of the same day, and across different days. We observed that the intensity of human traffic was much lower during the
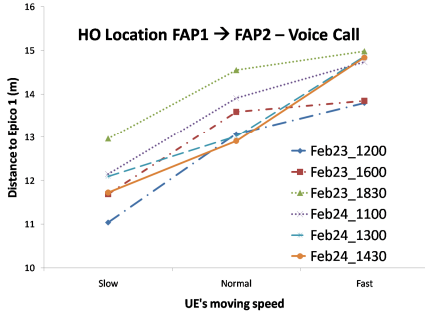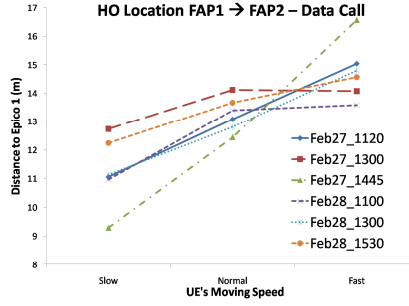
Figure 2: Handoff location for Voice call



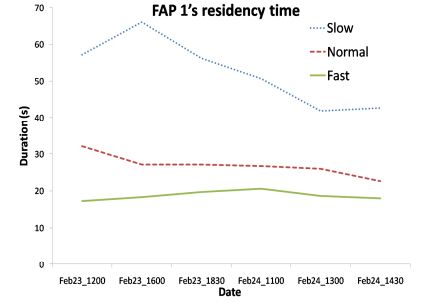Figure 3: Handoff location for Data call



Figure 4: Cell residency time for voice call

weekend than on a weekday. From the measured data, we derived the *handoff time* (and thus the residency duration of an individual cell), *handoff sequence* and *data throughput* at different movement speeds.

**Handoff Behavior:** Figures 2 and 3 illustrative the observed *representative behavior*, in terms of the distance of the handoff point from the current serving FAP (i.e., the implicit cell size), vs. the 3 different movement speeds, for different days (and different times within the same day). The figures illustrate the behavior for movements that cause transition from $FAP_1$ to $FAP_2$.

We observed the two following universal trends:

- The distance between the handoff location and the serving FAP increases when the participant's walking speed increases. As a corollary, the distance *to the target* FAP also decreases with an increase in the participant's movement speed. In general, it is well known that a faster moving mobile user will handoff at a greater distance from the center of the serving cell (as it will have moved farther in the period that the *time-to-trigger* threshold is exceeded). What is striking, however, is the magnitude of this variation– it varied by as much as 4m (for a voice call) and 7m (for a data session). This is an extremely significant difference, given that the nominal cell size of a FAP was around 10m, and this resulted simply from natural 'lifestyle-driven' changes in a participant's walking speed. Moreover, the increased distance also implies that the mobile node stays attached to a 'weaker signal' FAP for a longer duration; as we shall see shortly, this results in dramatic degradation in throughput.

- Besides the distance, the *handoff sequence* can also change with only modest changes in the participant movement speed. In particular, at higher movement speeds, the handoff skips an entire cell–e.g., in Figure 1a., handing off from $FAP_1$ directly to $FAP_3$ (instead of $FAP_2$). Policies for dynamic assignment of users between the femtocellular underlay and the macro overlay must, therefore, take into account this impact of movement speed on changing handoff patterns.

Taken together, these observations illustrate that even modest 'lifestyle driven' changes in movement speed can lead to dramatic changes in handoff behavior in indoor femtocellular environments, suggesting the need to incorporate such movement context in future dynamic subscriber management algorithms.

Figures 2 and 3 illustrate another equally important point: the handoff locations show significant longitudinal variation

(as much as $\approx$ 4m), under identical movement behavior, for different times of the day, and different days. Moreover, the handoff location is seen to depend on whether the active application is engaged in a voice-call or data-call. This variation is due to the fluctuations in the indoor RF propagation environment, suggesting the need for mechanisms to get more accurate, near-real time RF estimates.

As an alternative representation, Figure 4 plots the residency-time (the total time the user stays attached to $FAP_1$), while the user is in a voice call, at 6 different times. It can be seen that in the case of a slow walk, the residency times can vary longitudinally by as much as 25 to 30s. Fast and normal walk show lesser variation ($< 10s$), as the entire duration of walk is much smaller compared to slow walk.

**Throughput Behavior:** We also studied the changes in data throughput as a function of movement speed. Figures 5 and 6 plot the variation in throughput (and the serving cell ID) as a participant walks around at slow & fast movement speeds, respectively. The figures show a **very dramatic (6-8 fold) drop in throughput** as the walking speed increases! The dramatic degradation for these TCP data flows results from the longer period of 'poor connectivity' experienced by the mobile device. The poorer link quality and the more frequent incidence of handoffs lead to greater TCP packet losses and consequent TCP timeouts. Indeed, we can also observe that a handoff event (occuring when the serving cell ID changes) always results in a temporary (and sometimes very steep) dip in the application throughput.

In Fig 7, we plot the average throughput (total bytes transferred/ total walking time) for the entire walk, as a function of different speeds, and for different time-of-the-day/days. Clearly, the average throughput drops from a healthy 1.8Mbps to only 400-600 Kbps when the walking speed increases modestly. Moreover, the average throughput also shows appreciable variability (by as much as 200+ Kbps) across different days, reinforcing the need for better real-time prediction of indoor RF conditions.

## 5. DYNAMIC RF SIGNAL PREDICTION

Having motivated the need to accurately estimate the signal strength vectors (i.e., the RF map) in near-real time, as a precursor to handoff and throughput prediction, we now describe our initial work on dynamic RF prediction. In general, the measured RF signal from a FAP at any location is subject to a variety of attenuation affects, including: *a) Free space loss*, where the signal power is diminished by the outward geometric propagation of the waveform, *b) Atten-*
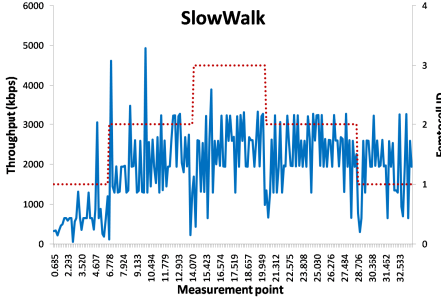
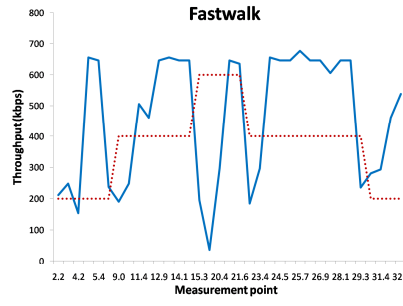Figure 5: Femtocell throughput and handoff Slow Walk



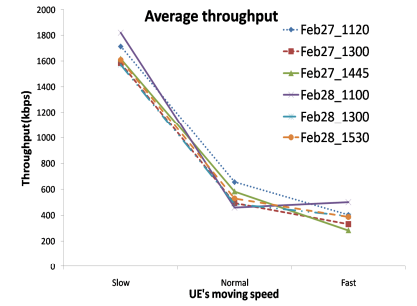Figure 6: Femtocell throughput and handoff Fast Walk



Figure 7: Average throughput for different walking speeds

uation, due to the signal traversing solid objects such as walls, window and the floors of buildings, *c) Scattering*, also known as multipath, that results from the reflection off surfaces in the indoor environment, and *d) Link Margin*, which reflects the quality (such as antenna gain) of the measurement equipment being used.

For the testbed measurements and results reported in this paper, we ignore the effects of Link Margin (which effectively gets subsumed into the $R$ term below), as all measurements are performed on the same device. In this case, we model the RF propagation in indoor environments using the well-known log-distance path loss mode (LDPM) as follows:

$$P_{ij} = P_i - 10\alpha_{ij} \log d_{ij} + R_{ij} \qquad (1)$$

In Eqn. 1, the mobile node $j$, also called the user equipment (**UE**), denoted by $UE_j$, located at a distance $d_{ij}$ (in meters) from $FAP_i$ observes a signal strength (RSCP) of $P_{ij}$ (measured in dBm). Here, $P_i$ is the received signal code power (RSCP) of $FAP_i$ at a distance of one meter, while $\alpha_{ij}$ is the exponent path loss coefficient (often observed to be between 3-4 indoors) that captures the combined free space loss & attenuation effects. $R_{ij}$ is a random variable that tries to capture the variation in RSCP due to scattering effects; in general, both $\alpha_{ij}$ and $R_{ij}$ depend on both transmitter and receiver locations and are affected by the internal building layout. We believe that the indoor environment should be partitioned into different zones, characterized by different value of $[\alpha, R]$. Thus, our model is different from EZ [7] model, which uses single $\alpha_i$ for each $FAP_i$ across the entire environment.

In this study, we assume that we know the transmit power $P_i$ (=100 mW) and 3-D location for each FAP and *the true distances for each (UE, AP) combination*. These assumptions will be relaxed for our future work, when weâĂŹ will apply ongoing work in indoor localization to *estimate* the location of the UEs. To construct the real-time RF map at any given location (indexed by $j$), we then need to compute the $(\alpha_{ij}, R_{ij})$ map for each FAP. Our current investigation assumes a crowd-sourced model, where UEs located at specific locations report their RSCP vectors to a central server: the central server's goal then is to *predict the RSCP vectors at other locations*, effectively by estimating the $(\alpha_{ij}, R_{ij})$ tuples for those locations. Our eventual goal (not addressed in this paper) is to establish the accuracy to which the server can delineate the cell boundaries for each FAP and predict the handoff locations for different movement speeds. We currently address two research questions:

- What algorithm do we use to estimate the $(\alpha_{ij}, R_{ij})$ tuples, and what is the *estimation error* that we observe?

- How does the estimation error vary with the number of observation samples vs. number of unobserved locations? This question effectively will help us understand how the accuracy degrades when the number of UEs reporting their measured RSCP values drops, and thus establishes the limits under which crowd-sourcing may be useful.

## 5.1 The RF Prediction Algorithm

Assume that there are $m$ FAPs and $n$ UEs and that the distances $d_{ij}$ are known. $UE_j$ reports to a server its observed RSCP vector $[P_{1j}, P_{2j}, , P_{mj}]$. Our prediction algorithm has two phrases: *clustering* and *parameter estimation*. In the clustering phase, the goal is to identify the physical regions that have the same (or similar) propagation effects (i.e., can be associated with a single $(\alpha_{ij}, R_{ij})$ value) and group them in the same 'logical' cluster. Subsequently, the parameter estimation phase determines the "best possible" estimates for $(\alpha_{ij}, R_{ij})$ values, independently for each cluster. The algorithms work as follows:

- *Clustering*: For each UE, we create the $2m$ dimensional feature vector, consisting of the $m$ UE-FAP distances and RSCP values–i.e., for $UE_j$, we obtain a $2m$ dimensional vector $[(d_{1j}, d_{2j}, \ldots, d_{mj}, P_{1j}, P_{2j}, \ldots, P_{mj}]$. We then cluster these points in the $2m$ dimensional space using the well known Expectation Maximization (EM) [8] algorithm. (Note that, in our approach, the number of clusters formed is not pre-specified but computed by the EM algorithm.) Our rationale is that UEs with similar distance and RSCP vectors should have similar $(\alpha, R)$ values, and should thus belong to the same logical group.

- *Parameter Estimation*: We now estimate the common $(\alpha, R)$ tuple for each cluster. We assume that each cluster is characterized by the same $2m$ dimensional vector $[(\alpha_1, R_1), (\alpha_2, R_2), , (\alpha_m, R_m)]$ vector. Assume the number of UE in a cluster is $k$; we then need to solve $k * m$ LDPL equations to find the $2 * m$ values $(\alpha, R)$. While there are several different approaches to solving this set of over-determined equations, in our implementation, we attempt to find a solution that
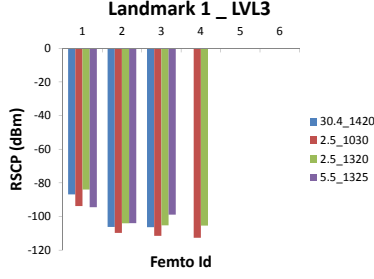
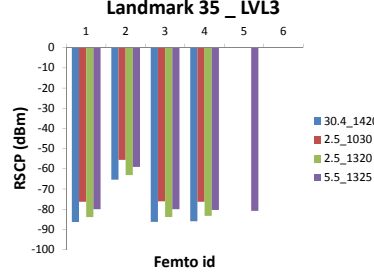Figure 8: Temporal RSCP Variation at Landmark 1 on Level 3



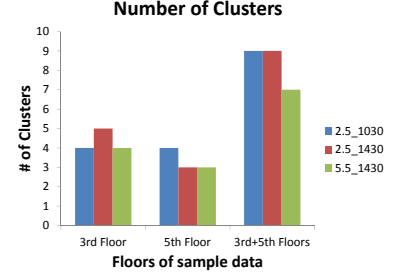Figure 9: Temporal RSCP Variation at Landmark 35 on Level 3



Figure 10: Temporal Variation of number of Cluster

minimizes the least mean absolute error,

$$J = \sum_{i=1}^{m} \sum_{j=1}^{k} \mid P_{ij} - P_i + 10\alpha_i \log d_{ij} - R_i \mid \quad (2)$$

Adapting the approach in [7], we use a Genetic algorithm (GA) [3] technique that efficiently searches the non-linear solution space efficiently to solve the set of LDPL equations. We then repeat the process to find the $(\alpha, R)$ tuple for all the other clusters generated in phase one.

## 5.2 Performance Results

For the experiments in this paper, we do not focus on actually implementing a real-time RF prediction solution. Instead, our goal is to use measurements (on different days) of the RSCP vectors (at the 57 sample points on the $3^{rd}$ floor and 40 sample points on $5^{th}$ floor) to understand the efficacy and accuracy bounds observed by our proposed algorithm.

### 5.2.1 Temporal Variation

We first note that there is, in fact, observable temporal variation in the RSCP measurements at the same location. Figures 8 and 9 present the temporal variation of RSCP at two landmarks on the $3^{rd}$ floor. The observed temporal variation in RSCP of FAP signals is as much as *15 dBm.* In the extreme case at landmark 35, the signal from $FAP_5$ is only available on one day of experiment on May $5^{th}$, and is not visible on the other days of experiments. Such temporal variation arises due to dynamic and unpredictable changes in a building's environmental and layout conditions.

Due to such temporal variation of RSCP values, the number of clusters computed by the EM algorithm vary across different days. Figure 10 plots the number of distinct clusters computed by our algorithm (at 2 different times on May $2^{nd}$ and also on May $5^{th}$), both separately for the $3^{rd}$ and $5^{th}$ floors and for a combination of both floors. Figure 11 presents the 4 clusters of $3^{rd}$ floor on May $5^{th}$.

### 5.2.2 RSCP Modeling Accuracy

We first study the ability of our model-based approach to accurately reconstruct the underlying RF measurements. Table 1 presents the differences between the measured RSCPs and the predicted RSCPs of all FAPs across all the landmarks. The table illustrates the maximum, minimum and mean prediction errors for the 3 time instants (2 on May $2^{nd}$ and1 on May $5^{th}$) under two different models: *a)* In the Real-time model, the RSCP readings from only that specific time in-
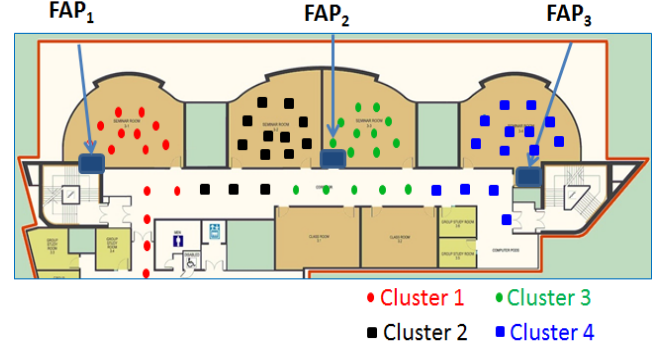


Figure 11: Sample clustering result on 3rd floor

stant are used by our 2-step estimation algorithm, while *b)* In the Static model, the clustering and estimation is done based on the average of all the observed readings across different days. In other words, the Real-time model generates different $(\alpha, R)$ values for different time instants, whereas the Static model generates a single $(\alpha, R)$ value, independent of time.

We see that the **mean** error for real-time estimation is 3.3 dBm, indicating that our estimation process provides significantly more accuracy than the temporal variation of 15dBm. Our mean prediction error also contrasts favorably against the **mean** error of 5.4 dBm achieved by the static model. More importantly, we computed the difference between the $95^{th} - 5th$ percentile of the estimation errors: this turned out to be only 12.5 dBm for the Real-time model, as compared to 24.6 dBm for the Static model. Our results demonstrate that our real-time prediction process is capable of making fairly accurate estimates of the RSCP vectors for unobserved locations. There are, however, a few locations where the prediction error is as high as 33 dBm, indicating that our model still needs additional fine-tuning. Our real-time estimation algorithms (including the clustering and GA phases) needed approximately 2 mins to execute on a consumer-grade laptop, indicating the computational feasibility of our approach.

### 5.2.3 Predicting Unknown Values based on Partial Observations

We now study how the estimation error varies with the relative proportion of observation samples vs. the number of unobserved points where the RSCP must be estimated. For all our results, we have used a 10-fold cross validation approach, where the sampled data set is randomly parti-

Table 1: Evaluation

| | Date of Exp | 2 May, 10:30 | | | 2 May, 14:30 | | | 5 May, 14:30 | | |
|---|---|---|---|---|---|---|---|---|---|---|
| | Floor | 3rd | 5th | 3rd +5th | 3rd | 5th | 3rd +5th | 3rd | 5th | 3rd +5th |
| **Real time** | Number of Cluster | 4 | 4 | 9 | 5 | 3 | 9 | 4 | 3 | 7 |
| | Min | 2E-4 | 3E-5 | 4E-5 | 6E-5 | 5E-4 | 3E-4 | 5E-6 | 5E-4 | 6E-5 |
| | Max | 25.695 | 18.848 | 20.656 | 12.911 | 22.34 | 22.693 | 33.719 | 28.585 | 32.906 |
| | Mean | 3.318 | 2.931 | 3.106 | 2.559 | 3.182 | 3.131 | 3.770 | 3.617 | 3.934 |
| | Standard Dev | 4.211 | 3.823 | 3.593 | 2.928 | 3.763 | 3.900 | 4.859 | 3.967 | 4.580 |
| **Static** | Number of Cluster | 4 | 4 | 8 | 4 | 4 | 8 | 4 | 4 | 8 |
| | Min | 5E-06 | 5E-4 | 1E-4 | 5E-6 | 9E-4 | 1E-4 | 5E-6 | 5E-5 | 1E-4 |
| | Max | 33.896 | 22.330 | 32.619 | 33.896 | 22.330 | 32.619 | 32.805 | 26.158 | 33.301 |
| | Mean | 5.724 | 4.317 | 5.284 | 5.719 | 5.019 | 5.617 | 5.532 | 4.500 | 5.307 |
| | Standard Dev | 7.657 | 4.973 | 6.685 | 7.542 | 5.378 | 6.784 | 7.432 | 4.952 | 6.624 |

tioned into 10 folds. To study the impact of changes in the fraction of observation samples, we then use $k$ folds for training our algorithm and the remaining (10-k) folds for testing the resulting model. The number of training data folds $k$ is varied from 9 to 1 to study the variation in the proportion of observation samples. Irrespective of the value of $k$, the experiments are repeated 10 times: each time, we randomly selects $k$ out of the 10 folds for training the model and the remaining $(10 - k)$ folds for testing. The overall estimation error (for each chosen value of $k$) is then obtained by averaging the results of these 10 different runs.

The training data set ($k$ folds), containing all the sample points with observed RSCP, is used to train the model with our proposed 2-phase algorithm, presented in section 5.1. For all the sample points in the testing data set $(10-k$ folds), we will predict the RSCP vectors $[P_{1j}, P_{2j}, \ldots, P_{mj}]$ based on their known distance vectors to the FAPs $[(d_{1j}, d_{2j}, \ldots, d_{mj}]$. The validation works as follows:

- *Predicting cluster membership*: For each testing point, find the top-5 nearest sample points from the training data set. The cluster membership of the testing point is determined by the majority vote from the cluster membership of the 5 training points. If all the 5 training points belong to 5 different clusters, the cluster membership of the nearest training point will be selected as the cluster membership for the testing point.

- *RSCP estimation*: After defining the cluster membership of the testing point, we use the estimated parameters of that cluster $[(\alpha_1, R_1), (\alpha_2, R_2), , (\alpha_m, R_m)]$ to estimate the expected RSCP vector $[P_{1j}, P_{2j}, \ldots, P_{mj}]$ by using the equation 1

We applied this 10-fold cross validation model, both independently for the $3^{rd}$ floor (57 sample points), $5^{th}$ floor (40 sample points) and also the combination of both floors (97 sample points). Figure 12 plots the average estimation error of the RSCP values (in dBm) for different values of $k$. Clearly, as expected, the average RSCP estimation errors increases as the number of training data sets or observation samples decrease. In general, it appears that values of $k = 9$ to 6 provide only marginal increase in the error, suggesting **that the crowd-sourced based estimation process works quite well when RSCP observations are available from mobile devices at $\approx 60\%$ of the total current sampled locations.** It is also worth noting

that the RSCP estimation error for a combined model across both floors is worse (higher) than when each floor is modeled separately. This suggests that, in practice, we should model each floor separately, to take into account the differences in propagation characteristics across floors.
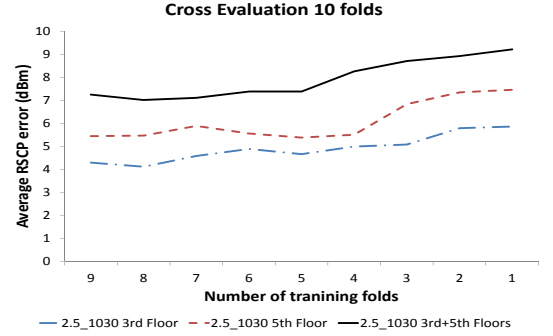


Figure 12: Cross Validation with 10 folds

# 6. CONCLUSION

This work represents a preliminary testbed-based investigation into the unique properties of femtocellular networks, especially in densely populated indoor environments, so that we can develop effective strategies for individualized, context-aware management of subscribers jointly across a femto-cum-macro cellular network. An initial set of longitudinal observation data demonstrates that the handoff process in such small-sized cellular environments is strongly influenced (handoff locations can change by 70% of a cell's radius) by even modest changes in pedestrian movement speed, and that the data throughput (at least for TCP flows) drops dramatically (as much as 8-fold) at higher speeds. More importantly, these variations are seen to have strong temporal dependency, thus suggesting the need for a mechanism that can use observational signal strength readings from selected locations to construct a dynamic RF propagation map and predict signal strength variations at other locations. Our proposed clustering-cum-optimization technique for signal strength estimation shows promise, as it incurs a mean error of $\approx 3$ dBm and works when RF 'ground truth' is observed at 60% or more of the indoor location landmarks.

In ongoing work, we are investigating several important and unresolved issues. First, we have to understand the sensitivity of our eventual metrics (handoff parameters and data throughput) to the RSCP prediction error—in other words, build predictive classifiers and then study the questions of 'how accurately can we predict handoff and throughput variation?', and 'how does this accuracy degrade with a reduction in observational samples?' Second, we have to deal with the practical reality that the indoor location reports are themselves only approximate, and more importantly, the location computation *itself depends on accurate models of RF attenuation.* In other words, there is a 'coupling' between RF propagation and location estimation that we need to address.

## 7. REFERENCES

[1] Livelabs urban lifestyle innovation platform. `http://www.livelabs.smu.edu.sg/`, 2012.

[2] Nemo outdoor 5.8. `http://www.anite.com/`, 2012.

[3] W. Banzhaf, F. D. Francone, R. E. Keller, and P. Nordin. *Genetic programming: an introduction: on the automatic evolution of computer programs and its applications.* Morgan Kaufmann Publishers Inc., San Francisco, CA, USA, 1998.

[4] Z. Becvar and P. Mach. Adaptive hysteresis margin for handover in femtocell networks. In *ICWMC'10*, 2010.

[5] V. Chandrasekhar, J. Andrews, and A. Gatherer. Femtocell Networks: A Survey. In *IEEE Communications Magazine*, volume 46, pages 59–67, 2008.

[6] V. Chandrasekhar, J. Andrews, T. Muharemovic, and Z. Shen. Power control in two-tier femtocell networks. In *IEEE Transactions on Wireless Communications*, Aug. 2009.

[7] K. Chintalapudi, A. P. Iyer, and V. Padmanabhan. Indoor localization without the pain. In *ACM MobiCom*, 2010.

[8] A. P. Dempster, N. M. Laird, and D. B. Rubin. Maximum likelihood from incomplete data via the em algorithm. *Journal of the Royal Statistical Society, Series B*, 39(1):1–38, 1977.

[9] Y. Gwon and R. Jain. Error characteristics and calibration-free techniques for wireless lan-based location estimation. In *ACM MobiWac*, 2004.

[10] Y. Ji, S. Biaz, S. Pandey, and P. Agrawal. Ariadne: A dynamic indoor signal map construction and localization system. In *ACM MobiSys*, 2006.

[11] K. Yeung and S. Nanda. Channel management in microcell/macrocellcellular radio systems. In *IEEE Trans. On Vehicular Technology*, Nov. 2006.

[12] J. Yun and K. Shin. Ctrl: A self-organizing femtocell management architecture for co-channel deployment. In *ACM Mobicom*.

[13] H. Zhang, X. Wen, W. Wang, B. Zheng, and Y. Sun. A novel handover mechanism between femtocell and macrocell for lte based networks. In *ICCSN'10*, 2010.